Inorganic Chemistry
Article

Mechanisms of Zn[II]-Activated Magnetic Resonance Imaging Agents

Jody L. Major, Rene M. Boiteau, and Thomas J. Meade*

Department of Chemistry, Biochemistry and Molecular Cell Biology, Neurobiology and Physiology, and Radiology, Northwestern University, 2145 Sheridan Road, Evanston, Illinois 60208-3113

We report on the mechanism of a series of Zn[II]-activated magnetic resonance contrast agents that modulate the access of water to a paramagnetic Gd[III] ion to create an increase in relaxivity upon binding of Zn[II]. In the absence and presence of Zn[II], the coordination at the Gd[III] center is modulated by appended Zn[II] binding groups. These groups were systematically varied to optimize the change in coordination upon Zn[II] binding. We observe that at least one appended aminoacetate must be present as a coordinating group to bind Gd[III] and effectively inhibit access of water. At least two binding groups are required to efficiently bind Zn[II], creating an unsaturated complex and allowing access of water. [13]C isotopic labeling of the acetate binding groups for NMR spectroscopy provides evidence of a change in the metal coordination of these groups upon the addition of Zn[II] supporting our proposed mechanism of activation as presented.

Introduction

Magnetic resonance imaging (MRI) is a noninvasive technique capable of producing three-dimensional images of opaque organisms with excellent spatial and temporal resolution.[1] MRI measures the ^{1}H NMR signal of water, where the signal intensity is proportional to the relaxation rates of the nuclear spins. Variation in the water concentration and local environment contributes to the vivid contrast observed in an acquired image. Intrinsic contrast can be augmented by employing paramagnetic contrast agents that are designed to accelerate the relaxation of water protons.[1,2] Typically, Gd[III] chelates are used as a result of having seven unpaired electrons and a symmetrical S ground state. The efficiency of these complexes to decrease the T_1 of water protons is reported by the relaxivity value, r_1 (mM^{-1} s^{-1}).[1,2]

The Solomon−Bloembergen−Morgan theory describes several variables that can be manipulated to produce changes in the relaxivity of a Gd[III] chelate and include the hydration number (q), the mean residence lifetime of coordinated waters (τ_m), and the rotational correlation time (τ_r).[3,4] In order to image biological processes in vivo, our laboratory pioneered the development of a series of activated contrast agents sensitive to enzymatic activity and secondary messengers.[5−10] These activated contrast agents exploit the modulation of coordinated water molecules to produce distinct relaxation states in response to a physiological event. Ideally, a q-modulated MRI contrast agent has two distinct states, a low relaxivity state ($q = 0$) before activation and a high relaxivity state ($q = 1$ or 2) after activation, to produce an increase in the observed MRI signal intensity.

Zn[II] plays a critical role in cellular physiology and is involved in structural stability, catalytic activity, and signal transduction processes.[11−13] The release of high concentrations of Zn[II] (200−300 μM) from neuronal synaptic vessels

* To whom correspondence should be addressed. E-mail: tmeade@ northwestern.edu.

(1) Merbach, A.; Toth, E. *The Chemistry of Contrast Agents in Medical Magnetic Resonance Imaging*; John Wiley & Sons, Ltd.: New York, 2001.
(2) Caravan, P.; Ellison, J. J.; McMurry, T. J.; Laufer, R. B. *Chem. Rev.* **1999**, *99*, 2293–2352.
(3) Solomon, I. *Phys. Rev.* **1955**, *99*, 559–565.
(4) Bloembergen, N.; Morgan, L. O. *J. Chem. Phys.* **1961**, *34*, 842–850.
(5) Li, W.-H.; Fraser, S. E.; Meade, T. J. *J. Am. Chem. Soc.* **1999**, *121*, 1413–1414.
(6) Li, W.-H.; Parigi, G.; Fragai, M.; Luchinat, C.; Meade, T. J. *Inorg. Chem.* **2002**, *41*, 4018–4024.
(7) Louie, A. Y.; Huber, M. M.; Ahrens, E. T.; Rothbacher, U.; Moats, R.; Jacobs, R. E.; Fraser, S. E.; Meade, T. J. *Nat. Biotechnol.* **2000**, *18*, 321–325.
(8) Duimstra, J. A.; Femia, F. J.; Meade, T. J. *J. Am. Chem. Soc.* **2005**, *127*, 12847–12855.
(9) Urbanczyk-Pearson, L. M.; Femia, F. J.; Smith, J.; Parigi, G.; Duimstra, J. A.; Eckermann, A. L.; Luchinat, C.; Meade, T. J. *Inorg. Chem.* **2008**, *47*, 56–68.
(10) Urbanczyk-Pearson, L. M.; Meade, T. J. *Nat. Protoc.* **2008**, *3*, 341–350.
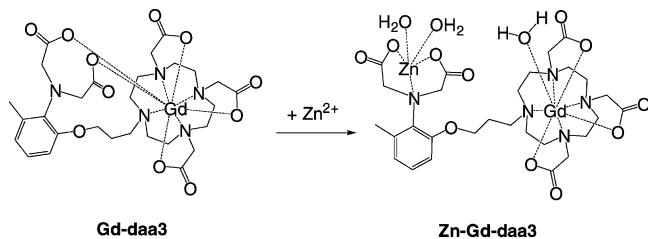(11) Takeda, A. *Brain Res. Rev.* **2000**, *34*, 137–148.
(12) Stefanidou, M.; Maravelias, C.; Dona, A.; Spiliopoulou, C. *Arch. Toxicol.* **2006**, *80*, 1–9.

Figure 1. Proposed mechanism of the Zn^{II}-activated MRI contrast agent **Gd-daa3**.

Figure 2. Complexes **1**−**4** with systematic variation of the aminoacetate and pyridyl Zn^{II}-coordinating groups.

into the extracellular fluids of the brain has been implicated in a variety of pathological pathways.[14] For example, Zn^{II} release has been implicated in the precipitation of β-amyloid plaques found in Alzheimer's disease.[15,16] The development of Zn^{II}-activated MRI contrast agents could provide a valuable tool in the study of in vivo Zn^{II} activity without using optical agents whose detection is limited by light scattering and photobleaching.[17−19]

Recently, we reported a Zn^{II}-activated MRI contrast agent where the relaxivity increases upon Zn^{II} binding.[20] Our proposed mechanism suggests that a pair of appended diaminoacetate arms bind to the Gd^{III} ion to create a coordinatively saturated complex ($q = 0$; Figure 1). In the presence of Zn^{II}, the diaminoacetates preferentially bind Zn^{II} and produce a change in the coordination geometry around the Gd^{III} center, producing an unsaturated complex and resulting in an increase in relaxivity. On the basis of a reported crystal structure of a diaminoacetate Zn^{II}-coordination derivative,[21] a distorted square-based pyramidal structure for Zn^{II} binding to the contrast agent is proposed. Coordination of Zn^{II} results in the formation of two five-membered rings sharing the Zn−N bond and can be described as an intermediate between square-based pyramidal and trigonal-bipyramidal geometries. The internal rearrangement of the diaminoacetate binding groups upon binding of Zn^{II} results in an increase of over 100% in the observed relaxivity of the agent.

Gd-daa3 has seven coordinating atoms available from the macrocyclic chelate and two aminoacetate ligands to bind Gd^{III}, resulting in a coordination number of nine. Considering **Zn-Gd-daa3**, it is possible for one or both aminoacetates to bind Zn^{II}. If both aminoacetate arms participate in Zn^{II} binding, two water molecules are expected to bind to the Gd^{III} ion. However, the experimentally determined q for **Zn-**
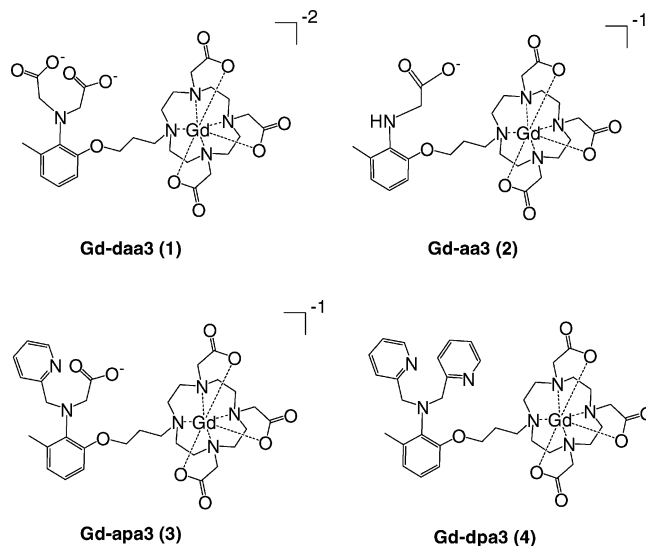
Gd-daa3 is 1.[20] This result raised the question concerning the coordination geometry of the aminoacetate pendant arms of **Gd-daa3** in the presence and absence of Zn^{II}.

Here, we investigate the coordinating groups of a series of Zn^{II}-activated agents to determine the role of binding and to prepare agents with a range of Zn^{II} binding (Figure 2). The systematic variation of Gd^{III}-coordinating aminoacetate groups and noncoordinating pyridyl groups allowed an investigation of the coordination geometry of **Gd-daa3**. We have discovered that while only one aminoacetate arm is necessary to efficiently block water to create a coordinatively saturated Gd^{III} complex, at least two binding groups are necessary for the binding of Zn^{II}. Therefore, it is possible to vary one of the aminoacetate arms to effectively tune the contrast agent to increase the selectivity and sensitivity for Zn^{II} activation.

Experimental Methods

Materials. GdCl$_3$·6H$_2$O, EuCl$_3$·6H$_2$O, TbCl$_3$·6H$_2$O, and 1,4,7,10-tetraazacyclododecane (cyclen) were purchased and used as is from Strem Chemicals (Newburyport, MA). Isotopically labeled 1,2-^{13}C-ethyl bromoacetate was purchased from Cambridge Isotope Laboratories, Inc. (Andover, MA). All other chemicals were purchased and used as is from Sigma-Aldrich. CH$_2$Cl$_2$, tetrahydrofuran (THF), and MeCN were dried using a solvent system purchased from Glass Contour, San Diego, CA. Water was purified using a Millipore Milli-Q synthesis water system. NMR spectra were recorded on either Varian (Palo Alto, CA) Inova 400 MHz or Varian Inova 500 MHz instruments with deuterated chloroform or water as the solvent. Electrospray ionization mass spectrometry (ESI-MS) spectra were obtained on a Varian 1200 L single-quadrupole mass spectrometer. Differences in the calculated and found mass spectrometry data for some complexes are a result of the isotopic patterns of the Gd^{III} complexes and the ^{13}C-labeled complexes. To confirm the purity of the final complexes, elemental analysis was performed by Desert Analytics Laboratory (Tucson, AZ).

Synthesis. The synthesis and characterization of **Gd-daa3** was accomplished as previously described.[20] **Gd-aa3** is a side product from the synthesis of **Gd-daa3** that is collected from the semi-preparatory high-performance liquid chromatography (HPLC). The

(13) Frederickson, C. J.; Koh, J.-Y.; Bush, A. I. *Nat. Rev. Neurosci.* **2005**, *6*, 449–462.
(14) Vallee, B. L.; Falchuk, K. H. *Physiol. Rev.* **1993**, *73*, 79–118.
(15) Frederickson, C. J.; Cuajungco, M. P.; Frederickson, C. J. J. *Alzheimer's Dis.* **2005**, *8*, 155–160.
(16) Noy, D.; Solomonov, I.; Sinkevich, O.; Arad, T.; Kjaer, K.; Sagi, I. *J. Am. Chem. Soc.* **2008**, *130*, 1376–1383.
(17) Hanaoka, K.; Kikuchi, K.; Urano, Y.; Nagano, T. *J. Chem. Soc., Perkin Trans. 2* **2001**, 1840–1843.
(18) Hanaoka, K.; Kikuchi, K.; Urano, Y.; Narazaki, M.; Yokawa, T.; Sakamoto, S.; Yamaguchi, K.; Nagano, T. *Chem. Biol.* **2002**, *9*, 1027–1032.
(19) Zhang, X.-a.; Lovejoy, K. S.; Jasanoff, A.; Lippard, S. J. *Proc. Nat. Acad. Sci., U.S.A.* **2007**, *104*, 10780–10785.
(20) Major, J. L.; Parigi, G.; Luchinat, C.; Meade, T. J. *Proc. Nat. Acad. Sci., U.S.A.* **2007**, *104*, 13881–13886.
(21) Hidalgo, M. A.; Suarez-Varela, J.; Avila-Roson, J. C.; Martin-Ramos, J. D.; Romerosa, A. *Acta Crystallogr.* **1996**, *C52*, 810–812.

synthetic procedure and characterization for **Gd-dpa3** and **Gd-apa3** are described. DO3A-tris-*tert*-butyl ester was synthesized following literature procedures.[22]

1-(3-Bromopropoxy)-3-methyl-2-nitrobenzene (5). To a solution of 3-methyl-2-nitrophenol (3.0 g, 19.6 mmol) in 200 mL of dry acetonitrile under nitrogen was added 9.12 g (66.0 mmol) of anhydrous potassium carbonate. After the reaction turned bright red because of the deprotonation of the phenol (10 min), 5.96 mL (58.7 mmol) of 1,3-dibromopropane was added, and the reaction was allowed to proceed at reflux overnight. After cooling to room temperature, the reaction was filtered, and the filtrate was washed with ethyl acetate and concentrated via rotary evaporation. The oily product was brought up in 100 mL of ethyl acetate and washed once with water followed by brine. The organic layer was dried over Na_2SO_4, filtered, and concentrated. The crude product was purified on a silica gel column, eluting with 5% ethyl acetate in hexanes to yield **5** as a light-yellow oil (5.1 g, 95% yield). ^{1}H NMR (400 MHz, CDCl$_3$w/TMS): δ 7.23 (t, $J = 8$ Hz, 1H), 6.85 (d, $J = 8$ Hz, 1H), 6.81 (d, $J = 7.6$ Hz, 1H), 4.12 (t, $J = 5.6$ Hz, 2H), 3.48 (t, $J = 6.8$ Hz, 2H), 2.22 (s, 3H), 2.21 (m, 2H). ^{13}C NMR (400 MHz, CDCl$_3$ w/TMS): δ 149.9, 142.3, 130.9, 130.8, 123.1, 111.2, 66.8, 32.1, 29.0, 17.1. MS (ESI$^+$). Calcd for (M + H$^+$): *m/z* 273.0. Found: *m/z* 273.9.

{4,7-Bis[(*tert*-butoxycarbonyl)methyl]-10-[3-(3-methyl-2-nitrophenoxy)propyl]-1,4,7,10-tetraazacyclododec-1-yl}acetic Acid *tert*-Butyl Ester (6). In a 250 mL round-bottomed flask, 2.0 g (7.3 mmol) of **5** was dissolved in 50 mL of dry acetonitrile. DO3A-tris-*tert*-butyl ester (2.5 g, 4.9 mmol) and anhydrous potassium carbonate (3.4 g, 24.3 mmol) were then added, and the resulting mixture was refluxed for 2 days. The reaction was cooled to room temperature and filtered. The crude product was absorbed onto silica and purified on a silica gel column, eluting with 2% methanol in dichloromethane. A 66% yield (2.3 g, 3.2 mmol) of **6** was obtained as a light-yellow oil. ^{1}H NMR (500 MHz, CDCl$_3$ w/TMS): δ 7.24 (t, $J = 8$ Hz, 1H), 6.83 (d, $J = 8$ Hz, 1H), 6.81 (d, $J = 8$ Hz, 1H), 4.01 (t, $J = 6$ Hz, 2H), 3.58–2.32 (multiplicity, 24H), 2.23 (s, 3H), 1.92 (m, 2H), 1.38 (s, 27H). ^{13}C NMR (500 MHz, CDCl$_3$ w/TMS): δ 170.6, 170.3, 149.6, 142.0, 131.2, 130.9, 123.2, 111.5, 82.0, 81.8, 66.4, 56.8, 55.5, 53.8, 53.4, 52.6, 50.0, 49.8, 48.0, 28.1, 22.9, 17.0. MS (ESI$^+$). Calcd for (M + H$^+$): *m/z* 707.5. Found: *m/z* 708.5. Calcd for (M + Na$^+$): *m/z* 730.4. Found: *m/z* 730.5.

{2-Methyl-6-[3-(4,7,10-tris[(*tert*-butoxycarbonyl)methyl]-1,4,7,10-tetraazacyclododec-1-yl)propoxy]phenylamino}acetic Acid *tert*-Butyl Ester (7). Product **6** (1.5 g, 2.1 mmol) was dissolved in methanol and added to a flask preloaded with 10% palladium on carbon (wet) in catalytic conditions. The reaction was equipped with a hydrogen reactor at 3.0 bar. After 48 h, the reaction was removed from the hydrogen reactor and filtered through celite, rinsing several times with methanol. Reduction of the nitro group to the amine was confirmed by MS [ESI$^+$; *m/z* 678.5 (M + H$^+$)]. The resulting orange oil was dissolved in 25 mL of dry acetonitrile. To this was added anhydrous potassium carbonate (0.85 g, 6.2 mmol) followed by 0.7 mL (4.5 mmol) of *tert*-butyl bromoacetate. The reaction was refluxed for 4 days and followed by thin-layer chromatography (TLC) to monitor the reaction progression. After a new spot was observed on the TLC due to the addition of the second acetate arm, the reaction was cooled to room temperature and filtered. The crude product was absorbed onto silica and purified on a silica gel column, eluting with 2% methanol in dichloromethane. **7** was obtained as an orange oil in 25% yield. ^{1}H NMR

(400 MHz, CDCl$_3$ w/TMS): δ 6.66 (Ar, 3H), 3.89 (t, $J = 6$ Hz, 2H), 3.71 (s, 2H), 3.66 (s, 1H, N*H*), 3.39–2.26 (multiplicity, 24H), 2.22 (s, 3H), 1.91 (m, 2H), 1.38 (s, 27H), 1.32 (s, 9H). ^{13}C NMR (400 MHz, CDCl$_3$ w/TMS): δ 173.8, 172.8, 171.4, 170.7, 149.4, 137.1, 128.0, 124.0, 120.7, 109.8, 82.9, 82.6, 81.7, 80.6, 67.1, 57.3, 56.7, 53.9, 51.9, 50.5, 28.1, 26.6, 18.9. MS (ESI$^+$). Calcd for (M + H$^+$): *m/z* 791.5. Found: *m/z* 792.5. Calcd for (M + Na$^+$): *m/z* 814.5. Found: *m/z* 814.5.

({2-Methyl-6-[3-(4,7,10-tris[(*tert*-butoxycarbonyl)methyl]-1,4,7,10-tetraazacyclododec-1-yl)propoxy]phenyl}pyridin-2-yl-methylamino)acetic Acid *tert*-Butyl Ester (8). In 50 mL of dry acetonitrile, 0.4 g (0.5 mmol) of **8** was added followed by anhydrous potassium carbonate (0.28 g, 2.0 mmol) and 2-(bromomethyl)pyridine hydrobromide (0.26 g, 1.0 mmol). The reaction was refluxed overnight and then cooled to room temperature, filtered, and concentrated via rotary evaporation. The crude product was absorbed onto silica and purified on a silica gel column, eluting with 3% methanol in dichloromethane. **8** was collected in 30% yield (0.13 g, 0.15 mmol) as an orange oil. MS (ESI$^+$). Calcd for (M + H$^+$): *m/z* 882.6. Found: *m/z* 883.2. Calcd for (M + Na$^+$): *m/z* 905.6. Found: *m/z* 905.1.

{4-{3-[2-[Bis(pyridin-2-ylmethyl)amino]-3-methylphenoxy]propyl}-7,10-bis[(*tert*-butoxycarbonyl)methyl]-1,4,7,10-tetraazacyclododec-1-yl}acetic Acid *tert*-Butyl Ester (9). Product **6** (0.35 g, 0.5 mmol) was dissolved in methanol and added to a flask preloaded with 10% palladium on carbon (wet) in catalytic conditions. The reaction was equipped with a hydrogen reactor at 3.0 bar. After 48 h, the reaction was removed from the hydrogen reactor and filtered through celite, rinsing several times with methanol. Reduction of the nitro group to the amine was confirmed with MS [ESI$^+$; *m/z* = 678.5 (M + H$^+$)]. The product was concentrated and brought up in 30 mL of dry acetonitrile. To this solution was added anhydrous potassium carbonate (0.17 g, 1.3 mmol) followed by 2-picoyl chloride (0.15 g, 0.9 mmol). The reaction was refluxed for 5 days to ensure that both picoyl groups were added. After filtering and rinsing with ethyl acetate and methanol, the crude product was absorbed onto silica for column purification, eluting with 5% methanol in dichloromethane. **9** was obtained as a pale-orange oil (0.15 g, 37% yield). ^{1}H NMR (500 MHz, CDCl$_3$ w/TMS): δ 8.44 (d, $J = 4.5$ Hz, 2H), 7.54 (t, $J = 7.5$ Hz, 2H), 7.33 (d, $J = 7.5$ Hz, 2H), 7.08 (t, $J = 7$ Hz, 2H), 6.95 (t, $J = 8$ Hz, 1H), 6.68 (overlapping doublets, $J = 8$ Hz, 2H), 4.35 (s, 2H), 4.30 (s, 2H), 3.91 (t, $J = 6$ Hz, 2H), 3.2–2.2 (multiplicity, 24H), 2.17 (s, 3H), 1.95 (m, 2H), 1.42 (s, 27H). ^{13}C NMR (500 MHz, CDCl$_3$ w/TMS): δ 172.8, 160.0, 157.7, 148.9, 138.8, 137.6, 136.2, 126.2, 123.4, 123.0, 121.9, 109.8, 82.8, 82.5, 66.3, 60.2, 55.9, 51.6, 51.1–50.0 (overlapping cyclen peaks), 28.0, 25.6, 19.0. MS (ESI$^+$). Calcd for (M + H$^+$): *m/z* 859.6. Found: *m/z* 860.6. Calcd for (M + Na$^+$): *m/z* 882.5. Found: *m/z* 882.6.

Metalation Procedure. A trifluoroacetic acid (TFA) solution, 95:2.5:2.5 (TFA/ H$_2$O/ triisopropylsilane) was added to the protected ligands **8** and **9** for 12 h. After TFA was removed by purging the solution with air and 15 mL of diethyl ether was added, the precipitate was centrifuged and decanted. The diethyl ether wash was repeated twice, the final pellet was brought up in H$_2$O, and the pH was adjusted to 6.5 with 1 M NaOH. A total of 1.1 equiv of GdCl$_3$·6H$_2$O was then added, and the resulting mixture was stirred at room temperature for several days. Unreacted Gd^{III} precipitated as Gd(OH)$_3$ after the addition of 1 M NaOH to a pH of 10 and pelleted. The crude mixture was purified by semiprepra-tive HPLC on a reverse-phase column, eluting with acetonitrile and water using an isocratic ramp from 0% to 100% acetonitrile over 35 min. Analytical HPLC−MS was used to confirm the purity and

(22) Dadabhoy, A.; Faulkner, S.; Sammes, P. G. *J. Chem. Soc., Perkin Trans. 2* **2002**, 348–357.

identity of the collected fractions. Pure fractions were freeze-dried and stored in a desiccator. The same procedure was followed with TbCl$_3$·6H$_2$O to obtain the Tb^{III} metal complexes.

Gd-daa3. Gadolinium(III) Carboxymethyl-{2-methyl-6-[3-[4,7,10-tris(carboxymethyl)-1,4,7,10-tetraazacyclododec-1-yl]propoxy]phenylamino}acetic Acid (1). Analytical LC−MS showed a single peak (ESI$^+$). Calcd for (M + H$^+$): m/z 778.2. Found: m/z 781.2. Anal. Calcd for C$_{28}$H$_{38}$GdN$_5$O$_{11}$·2H$_2$O·2Na: C, 39.11; H, 4.93; N, 8.14. Found: C, 39.33; H, 4.93; N, 7.84. **Tb-daa3.** Analytical LC−MS showed a single peak (ESI$^+$). Calcd for (M + H$^+$): m/z 779.2. Found: m/z 779.2. Calcd for (M + Na$^+$): m/z 802.2. Found: m/z 801.2.

Gd-aa3. Gadolinium(III) {2-Methyl-6-[3-[4,7,10-tris(carboxymethyl)-1,4,7,10-tetraazacyclododec-1-yl]propoxy]phenylamino}acetic Acid (2). Analytical LC−MS showed a single peak (ESI$^+$). Calcd for (M + H$^+$): m/z 721.1. Found: m/z 720.2. Anal. Calcd for C$_{26}$H$_{38}$GdN$_5$O$_9$·H$_2$O·Na: C, 40.94; H, 5.29; N, 9.18. Found: C, 40.81; H, 5.27; N, 9.02.

Gd-apa3. Gadolinium(III) {{2-Methyl-6-[3-[4,7,10-tris(carboxymethyl)-1,4,7,10-tetraazacyclododec-1-yl]propoxy]phenyl}pyridin-2-ylmethylamino}acetic Acid (3). Analytical LC−MS showed a single peak (ESI$^+$). Calcd for (M + H$^+$): m/z 812.2. Found: m/z 813.0. Anal. Calcd for C$_{32}$H$_{42}$GdN$_6$O$_9$·2H$_2$O: C, 45.32; H, 5.47; N, 9.91. Found: C, 45.37; H, 5.79; N, 10.32. **Tb-apa3**. Analytical LC−MS showed a single peak (ESI$^+$). Calcd for (M + H$^+$): m/z 813.2. Found: m/z 814.2.

Gd-dpa3. Gadolinium(III) {4-{3-[2-[Bis(pyridin-2-ylmethyl)-amino]-3-methylphenoxy]propyl}-7,10-bis(carboxymethyl)-1,4,7,10-tetraaza-cyclododec-1-yl}acetic Acid (4). Analytical LC−MS showed a single peak (ESI$^+$). Calcd for (M + H$^+$): m/z 846.3. Found: m/z 847.2. Anal. Calcd for C$_{36}$H$_{47}$GdN$_7$O$_7$: C, 51.05; H, 5.59; N, 11.58. Found: C, 51.15; H, 5.61; N, 11.22. **Tb-dpa3**. Analytical LC−MS showed a single peak (ESI$^+$). Calcd for (M + H$^+$): m/z 847.3. Found: m/z 848.3.

***tert*-Butyldimethyl-[3-(3-methyl-2-nitrophenoxy)propoxy]silane (10).** To a solution of 3-methyl-2-nitrophenol (5.0 g, 32.6 mmol) in dry acetonitrile (300 mL) under nitrogen was added K$_2$CO$_3$ (11.26 g, 81.5 mmol). After the reaction had turned a bright-red color because of the deprotonated state of the phenol (about 10 min), (3-bromopropoxy)-*tert*-butyldimethylsilane (9.04 mL, 39.2 mmol) was added. The reaction was refluxed at 70 °C until it was a pale-yellow color, cooled to room temperature, and filtered. After evaporation of the solvent, the mixture was brought up in 100 mL of ethyl acetate and washed once with an aqueous saturated sodium bicarbonate solution and once with brine. The organic layer was dried over Na$_2$SO$_4$ and concentrated in vacuo. The residue was purified on a silica gel column, eluting with 1% ethyl acetate in hexanes, yielding **10** as light-yellow crystals after drying (10.11 g, 94% yield). ^{1}H NMR (500 MHz, CDCl$_3$ w/TMS): δ 7.27 (t, J = 8 Hz, 1H), 6.89 (d, J = 8.5 Hz, 1H), 6.84 (d, J = 8 Hz, 1H), 4.15 (t, J = 6 Hz, 2H), 3.75 (t, J = 6 Hz, 2H), 2.30 (s, 3H), 1.96 (m, J = 5.5 Hz, 2H), 0.88 (s, 9H), 0.04 (s, 6H). ^{13}C NMR (500 MHz, CDCl$_3$ w/TMS): δ 150.44, 142.43, 131.06, 130.76, 122.54, 111.01, 65.89, 59.15, 32.23, 26.11, 18.49, 17.17, −5.13, −5.41. MS (ESI$^+$). Calcd for (M + H$^+$): m/z 325.2. Found: m/z 326.2. Calcd for (M + Na$^+$): m/z 348.2. Found: m/z 348.1.

{{2-[3-(*tert*-Butyldimethylsilanyloxy)propoxy]-6-methylphenyl}ethoxycarbonylmethylamino}acetic Acid Ethyl Ester (11). In 30 mL of methanol, 1.0 g of **10** (3.07 mmol) was dissolved and added to a flask preloaded with 10% palladium on carbon (wet) in catalytic conditions. The reaction was equipped with a hydrogen reactor at 3.0 bar for 24 h. Upon completion of reduction, the reaction was filtered over celite, rinsed several times with 50 mL

methanol, and concentrated via rotary evaporation of the solvent. The resulting oil was transferred to a 100 mL round-bottomed flask and dissolved in dry acetonitrile (30 mL). Proton sponge (2.79 g, 13.0 mmol) was dissolved in the reaction mixture before the addition of 1.0 g (5.92 mmol) of 1,2-^{13}C-ethyl bromoacetate followed by sodium iodide (1.95 g, 13.0 mmol). After 2 days of refluxing, the reaction was filtered, rinsed with ethyl acetate, and concentrated via rotary evaporation. The crude product was absorbed onto silica and purified on a silica gel column, eluting with a slow gradient of 2% ethyl acetate in hexanes to 5% ethyl acetate. The desired product **11** was collected in 75% yield as a light-yellow oil. ^{1}H NMR (500 MHz, CDCl$_3$ w/TMS): δ 7.00 (t, J = 8 Hz, 1H), 6.79 (d, J = 7.5 Hz, 1H), 6.72 (d, J = 7.5 Hz, 1H), 4.12 (m, 4H), 4.05 (t, J = 6.5 Hz, 2H), 3.91 (s, broad, 2H), 3.85 (t, J = 6 Hz, 2H), 3.74 (s, broad, 2H), 2.47 (s, 3H), 2.04 (m, 2H), 1.24 (t, J = 7 Hz, 6H), 0.91 (s, 9H), 0.07 (s, 6H). ^{13}C NMR (500 MHz, CDCl$_3$ w/TMS): δ 172.5, 157.0, 139.3, 137.7, 126.4, 122.9, 109.7, 64.8, 60.5, 56.6, 49.8, 32.9, 26.2, 21.3, 18.6, 14.4, −5.1. MS (ESI$^+$). Calcd for (M + H$^+$): m/z 469.3. Found: m/z 472.3. Calcd for (M + Na$^+$): m/z 492.2. Found: m/z 494.3.

{(Ethoxycarbonyl)methyl-[2-(3-hydroxypropoxy)-6-methylphenyl]amino}acetic Acid Ethyl Ester (12). To a solution of **11** (1.1 g, 2.3 mmol) in THF (25 mL) was added tetrabutylammonium fluoride (1.5 g, 5.8 mmol). After 2 h at room temperature, the deprotection was completed as observed by TLC (1:3 EtOAc/hexanes). THF was removed via rotary evaporation. The crude product was brought up in ethyl acetate and washed once with water and then brine. The organic layer was dried over sodium sulfate, filtered, concentrated, and purified through a silica plug, eluting with 25% ethyl acetate in hexanes and yielding the desired product in 83% yield (0.68 g, 1.9 mmol). ^{1}H NMR (500 MHz, CDCl$_3$ w/TMS): δ 7.00 (t, J = 8 Hz, 1H), 6.80 (d, J = 8 Hz, 1H), 6.74 (d, J = 8.5 Hz, 1H), 4.14 (m, 6H, overlapping OCH_2CH$_3$ and OCH_2CH$_2$CH$_2$OH), 4.06 (s, broad, 2H), 3.90 (t, J = 5.5 Hz, 2H), 3.79 (s, broad, 2H), 2.45 (s, 3H), 2.08 (m, 2H), 1.23 (t, J = 7 Hz, 6H). ^{13}C NMR (500 MHz, CDCl$_3$ w/TMS): δ 172.5, 156.4, 138.5, 137.3, 126.1, 123.4, 110.1, 65.7, 60.2, 49.6, 32.4, 18.7, 14.4. MS (ESI$^+$). Calcd for (M + H$^+$): m/z 355.2. Found: m/z 358.2. Calcd for (M + Na$^+$): m/z 378.2. Found: m/z 380.1.

{[2-(3-Bromopropoxy)-6-methylphenyl]ethoxycarbonylmethyl-amino}acetic Acid Ethyl Ester (13). To a solution of **12** (0.5 g, 1.4 mmol) in dry methylene chloride (15 mL) was added carbon tetrabromide (0.7 g, 2.1 mmol) followed by the slow addition of triphenylphosphine (0.7 g, 2.8 mmol). After 2 h at room termperature, the reaction was washed with water and brine, dried over sodium sulfate, filtered, and concentrated. The crude product was purified on a silica gel column, eluting with 5% ethyl acetate in hexanes and giving **13** in 94% yield as an orange oil. ^{1}H NMR (500 MHz, CDCl$_3$ w/TMS): δ 7.01 (t, J = 8 Hz, 1H), 6.81 (d, J = 7 Hz, 1H), 6.73 (d, J = 8.5 Hz, 1H), 4.11 (m, 6H, overlapping OCH_2CH$_3$ and OCH_2CH$_2$CH$_2$Br), 4.00 (s, broad, 2H), 3.73 (s, broad, 2H), 3.67 (t, J = 6.5 Hz, 2H), 2.46 (s, 3H), 2.37 (m, 2H), 1.23 (t, J = 6.5 Hz, 6H). ^{13}C NMR (500 MHz, CDCl$_3$ w/TMS): δ 172.0, 156.5, 139.2, 137.6, 126.3, 123.5, 109.9, 65.7, 60.6, 56.3, 49.6, 32.7, 18.6, 14.5. MS (ESI$^+$). Calcd for (M + H$^+$): m/z 417.1. Found: m/z 420.0. Calcd for (M + Na$^+$): m/z 440.1. Found: m/z 442.0.

{Ethoxycarbonylmethyl-{2-methyl-6-[3-[4,7,10-tris[(*tert*-butoxycarbonyl)methyl]-1,4,7,10-tetraazacyclododec-1-yl)propoxy]-phenyl]amino}acetic Acid Ethyl Ester (14). To a solution of DO3A-tris-*tert*-butyl ester (0.55 g, 1.1 mmol) in 15 mL of dry acetonitrile was added anhydrous potassium carbonate (0.44 g, 3.2 mmol). After 5 min, a solution of **13** (0.55 g, 1.3 mmol) in 5 mL

Scheme 1. Synthesis of **Gd-apa3** (**3**) and **Gd-dpa3** (**4**)
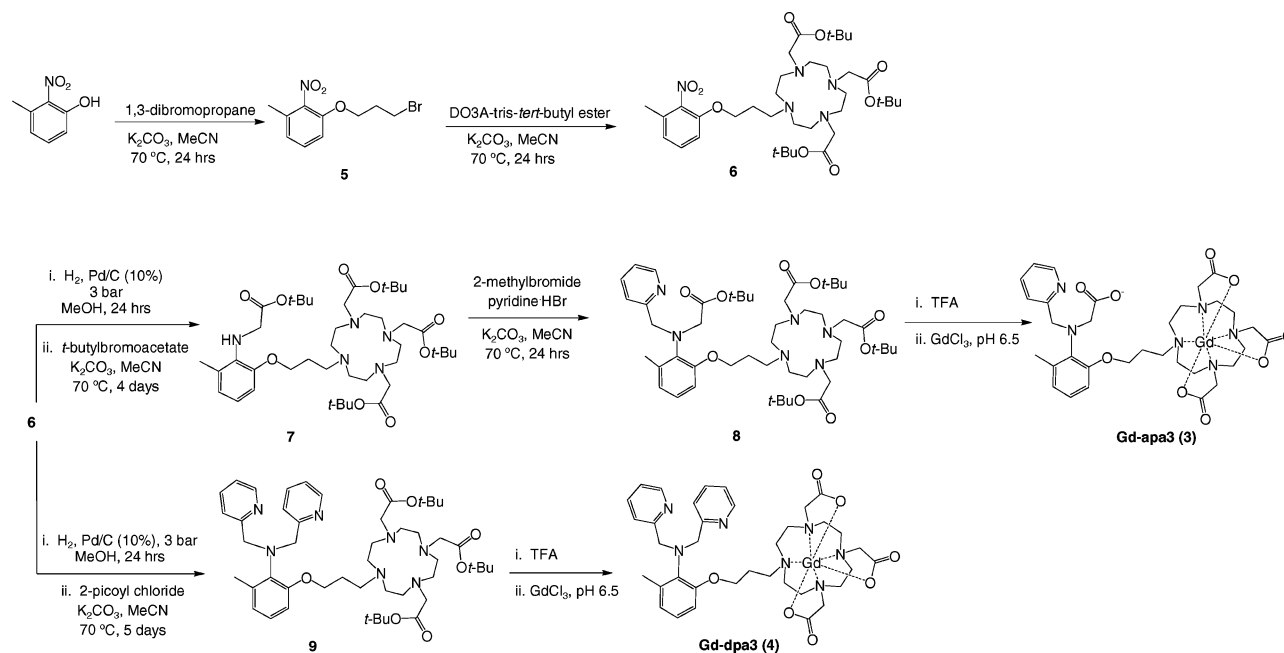
of dry acetonitrile was added to the reaction, and the mixture was refluxed overnight. The reaction was cooled and filtered, rinsing with acetonitrile followed by methanol. The solvents were removed by rotary evaporation, and the crude product was purified on a silica gel column, eluting with 3% MeOH in dichloromethane to yield **14** in 27% yield. After trituration with diethyl ether several times, a pale-yellow solid was obtained. ^1H NMR (400 MHz, CDCl$_3$ w/TMS): δ 6.91 (t, J = 8 Hz, 1H), 6.72 (d, J = 7.6 Hz, 1H), 6.62 (d, J = 8.4 Hz, 1H), 3.95−2.30 (multiplicity, 36H), 2.35 (s, 3H), 1.27 (s, 27H), 1.17 (m, 6H). ^{13}C NMR (500 MHz, CDCl$_3$ w/TMS): δ 172.6, 164.2, 156.4, 139.0,126.3, 123.3, 109.7, 82.9, 82.6, 66.5, 60.5, 55.8, 51.7, 50.7, 50.0, 49.8, 49.4, 49.2, 47.9, 28.1, 18.4, 14.4. MS (ESI$^+$). Calcd for (M + Na$^+$): m/z 874.5. Found: m/z 876.6.

Eu-daa3. Europium(III) Carboxymethyl-{2-methyl-6-[3-[4,7,10-tris(carboxymethyl)-1,4,7,10-tetraazacyclododec-1-yl]propoxy]phenylamino}acetic Acid (15). The protected ligand **14** was first reacted with 1.0 M NaOH for 24 h to deprotect the ethyl groups. After neutralization to a pH of 7, the crude product was freeze-dried and then brought up in a solution of TFA for 24 h. TFA was removed by purging the solution with air, and approximately 15 mL of diethyl ether was added. The precipitate was centrifuged and decanted. The diethyl ether wash was repeated two times, the final pellet was brought up in H$_2$O, and the pH was adjusted to 6.5 with 1 M NaOH. A total of 1.1 equiv of EuCl$_3$·6H$_2$O was added and stirred at room temperature for several days. Unreacted Eu^{III} precipitated as Eu(OH)$_3$ after the addition of 1 M NaOH, and the crude mixture was purified by semipreprative HPLC, eluting with acetonitrile and water. Analytical HPLC−MS was used to confirm the purity and identity of the collected fractions and showed a single peak with MS (ESI$^+$). Calcd for (M + H$^+$): m/z 772.6. Found: m/z 772.5.

Relaxivity Measurements. A 1 mM solution of each Gd^{III} complex was prepared in buffer containing 100 mM KCl/100 mM HEPES at pH 7.4. These were serially diluted four times to give 500 μL of five different sample concentrations at a [Gd]:[Zn] ratio of 1:0. Aliquots of a 5.0 mM ZnCl$_2$ solution in HEPES were added to each of the samples to give a [Gd]:[Zn] ratio of 1:0.5. After 30 min of incubation at 37 °C, T_1 measurements were performed on a Bruker mq60 minispec relaxometer with an inversion−recovery

pulse sequence with the appropriate recycle delays. The spectrometer fits 10 data points to an exponential decay for each T_1 measurement and calculates the standard deviation for each T_1, representing an error of less than 1%. This titration was repeated until a 1:3 ([Gd]:[Zn]) ratio was reached.

Luminescence Lifetime Measurements. The fluorescence decay rates of the terbium analogues of **1**, **3**, and **4** in buffered H$_2$O and D$_2$O were measured on a Hitachi F4500 fluorometer monitoring the emission at 544 nm with an excitation of 254 nm. Aliquots of HEPES buffer and ZnCl$_2$ in HEPES were freeze-dried before being brought up in D$_2$O to ensure there was no water present. A 200 μM solution of the terbium complex in HEPES buffer was measured in the presence of 300 μM ZnCl$_2$ and without ZnCl$_2$. A total of 25 scans were averaged and fit to a monoexponential decay with an r^2 value of 0.99.

Inductively Coupled Plasma Atomic Emission Spectrometry (ICP-AES). The concentration of each sample for relaxivity was determined by ICP-AES (Varian). A 10 μL aliquot of each sample was digested in 90 μL of nitric acid. Each sample was diluted with water to the appropriate concentration for ICP-AES analysis. Gadolinium concentrations were determined from a standardized curve of six standards ranging from 0 to 500 ppb Gd^{III}, measuring the emission of Gd^{III} at 335.048, 336.224, and 342.246 nm.

Results

Synthesis. The syntheses of **3** and **4** are outlined in Scheme 1. Starting with 3-methyl-2-nitrophenol, 1,3-dibromopropane was added using potassium carbonate in dry acetonitrile. DO3A-tris-*tert*-butyl ester was synthesized following literature procedures[22] and combined with **5** under basic conditions to yield **6**. The nitro group of **6** was then reduced under standard palladium-catalyzed hydrogenation conditions and reacted with either *tert*-butyl bromoacetate to yield **7** or with 2-picoyl chloride to yield **9**. The final pyridyl binding group was added to **7** using 2-bromopyridine hydrobromide to yield the final *tert*-butyl-protected ligand **8**. Both **8** and **9** were reacted with trifluoroacetic acid to

Scheme 2. Synthesis of ^{13}C-Isotopically Labeled **Eu-daa3** (**15**; * = [13]C)
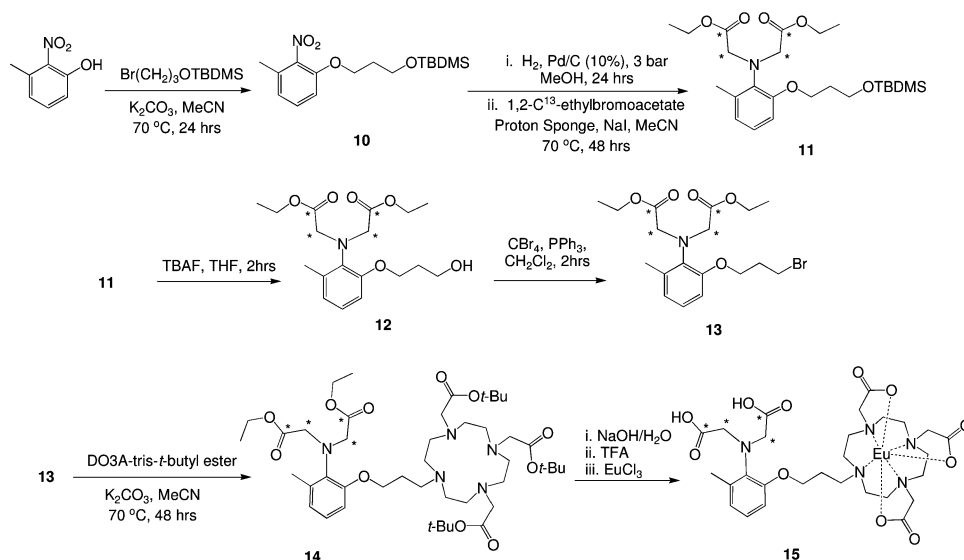
remove the *tert*-butyl protecting groups and reacted with GdCl3·6H2O at a pH of 6.5 for 2 days. The final compounds **3** and **4** were purified by semipreparatory HPLC and characterized by LC−MS and elemental analysis.

The ^{13}C isotopic labeling of the aminocarboxylates of **Gd-daa3** was synthesized following previously published procedures with some modifications outlined in Scheme 2.[20] The synthesis begins with alkylation of the commercially available 3-methyl-2-nitrophenol with the *tert*-butyldimethylsilyl-protected alcohol to give **10** in 95% yield. After standard hydrogenation conditions, the two aminoacetate arms were added using 1,2-^{13}C-ethyl bromoacetate in the presence of proton sponge and sodium iodide. Deprotection of the TBDMS protecting group was achieved with tetrabutylammonium fluoride to yield **12**, which was brominated with carbon tetrabromide in the presence of triphenylphosphine to give **13**. The addition of DO3A-tris-*tert*-butyl ester was achieved with potassium carbonate in acetonitrile under refluxing conditions to give the fully protected ligand **14**. The ethyl groups were deprotected through the addition of 1 M NaOH at room temperature. After neutralization, the *tert*-butyl groups were deprotected with TFA before the addition of the metal with EuCl3·6H2O. The final compound was purified by semipreparatory HPLC and characterized by analytical LC−MS.

Relaxivity. To evaluate the binding properties of the aminoacetate and pyridyl groups employed in complexes **1**−**4**, relaxivities were first measured in the absence of Zn^{II} at 60 MHz and 37 °C in HEPES buffer to determine the effectiveness in creating a coordinatively saturated Gd^{III} complex with low relaxivity. As seen in Table 1, the complexes with one or two aminoacetates are binding to Gd^{III} and thus create a low-relaxivity complex. The relaxivity of **Gd-dpa3** of 7.5 mM⁻¹ s⁻¹ illustrates the inability of the pyridyl nitrogen atoms to bind with Gd^{III} and therefore not reduce water access to the Gd^{III} ion. The lowest relaxivity observed is for **Gd-daa3**, suggesting that both aminoacetates participate in the binding of Gd^{III}, as depicted in Figure 1. The two complexes with only one aminoacetate, **Gd-aa3** and

Table 1. Relaxivity in the Presence and Absence of Zn^{II} at 60 MHz and 37 °C in HEPES Buffer

	r_1 (mM⁻¹s⁻¹)		
	0 equiv of Zn^{II}	1 equiv of Zn^{II}	% change in r_1
Gd-daa3	2.3	5.1	+ 121%
Gd-aa3	4.1	4.2	+ 2.4%
Gd-apa3	3.4	6.9	+ 103%
Gd-dpa3	7.5	7.2	− 4.0%

Gd-apa3, do not have as low of a relaxivity as that observed for **Gd-daa3**; however, they still have the ability to bind Gd^{III} and effectively reduce the access of water. This suggests that a coordination number of eight is sufficient in creating a coordinatively saturated Gd^{III} complex. The lower relaxivity for **Gd-apa3** compared to **Gd-aa3** may be due to the added steric effects in reducing water access from the second pyridyl arm of **Gd-apa3**. While there is no direct evidence from these experiments of the effect on second-sphere solvation, the presence of the noncoordinating pyridyl ligand may allow for the reduction of second-sphere water molecules, resulting in an overall decrease in the observed relaxivity.

In the presence of 1 equiv of ZnCl2 in HEPES buffer at 60 MHz and 37 °C, the relaxivities of both **Gd-daa3** and **Gd-apa3** increase by 121% and 103%, respectively, while there was no significant change in the relaxivity for **Gd-aa3** (Table 1). Importantly, **Gd-aa3** exhibits no increase in r_1 upon the addition of Zn^{II}, implying that there is no change in the coordination environment. This is the only complex with only one available binding group and, therefore, it is reasonable to suggest that two binding groups are required for coordinating Zn^{II}. Given that **Gd-dpa3** was not able to create a coordinatively saturated structure when no Zn^{II} was present, it was expected that there would be little change in its relaxivity with the addition of Zn^{II}, as observed.

Luminescence. The relaxivity studies presented suggest that, in the absence of Zn^{II}, complexes with at least one available aminoacetate arm to coordinate Gd^{III} have low relaxivity values, as would be expected for a $q = 0$ complex. While the relaxivity measurements reflect the effect of both
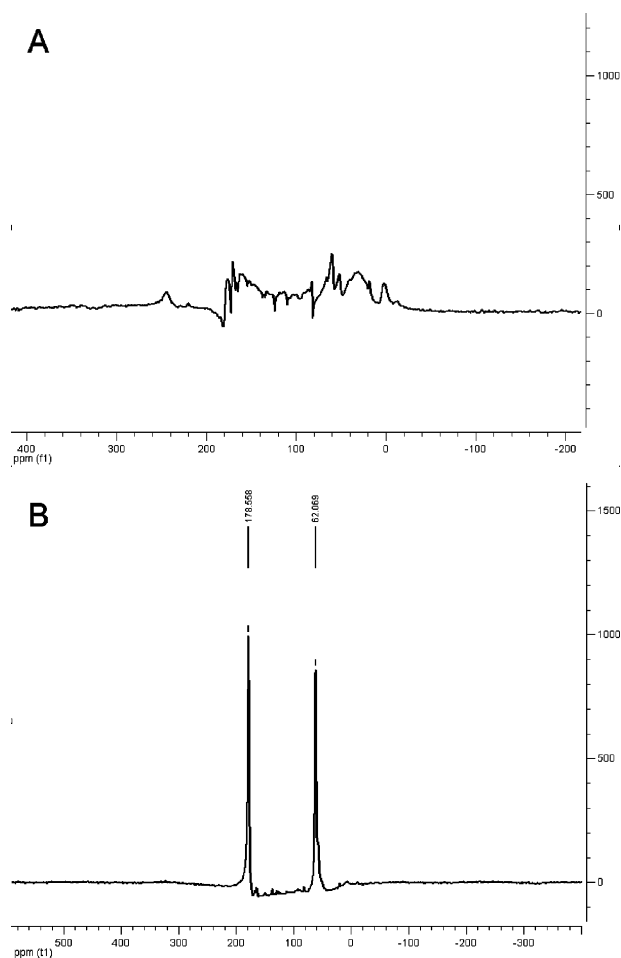
Table 2. Fluorescence Decay Lifetimes of **1**, **3**, and **4** in H_2O and D_2O and Their Calculated q Values

	τ_{H_2O} (ms)	τ_{D_2O} (ms)	q	τ_{H_2O} (ms) + Zn^{II}	τ_{D_2O} (ms) + Zn^{II}	q + Zn^{II}
1	1.97	2.71	0.3	1.46	2.65	1.0
3	1.76	2.21	0.2	1.63	2.67	0.8
4	1.21	2.33	1.4	1.18	2.33	1.5

the inner-sphere water molecules and the second solvation shell, fluorescence lifetime measurements can directly report on the first solvation sphere. To determine if, in fact, an eight-coordinate complex could provide a coordinatively saturated complex, the hydration numbers (q) of the terbium analogues of **1**, **3**, and **4** were determined using time-based fluorescence microscopy measurements. The fluorescence decay rates of the Tb^{III} analogues in water and D_2O with and without Zn^{II} present were measured to calculate q. Because of the efficient vibronic coupling of the Tb^{III} excited state to the O−H oscillators compared to that of the O−D oscillators, a shorter luminescence lifetime is observed in H_2O than in D_2O.[23] The number of coordinated water molecules is then calculated using eq 1.[24,25] The fluorescence lifetimes and calculated q values are summarized in Table 2. These measurements confirm a change in the coordination environment for **Gd-daa3** and **Gd-apa3** from a $q = 0$ complex to a $q = 1$ complex. The hydration numbers for **Gd-apa3** provide further evidence of an eight-coordination Gd^{III} complex. In the absence of Zn^{II}, the eight coordinating arms bind Gd^{III} with no open site for water access, while in the presence of Zn^{II}, there is one inner-sphere water molecule bound to Gd^{III} along with the seven coordinating groups from the chelate. The hydration numbers calculated for **Gd-dpa3** confirm that in the absence of Zn^{II} the pyridyl groups do not bind Gd^{III}. Therefore, the hydration number in the absence and presence of Zn^{II} remains unchanged.

$$q = 4.2 \text{ ms} \left[\left(\frac{1}{\tau_{H_2O}} \right) - \left(\frac{1}{\tau_{D_2O}} \right) - 0.06 \right] \qquad (1)$$

Europium ^{13}C NMR Spectroscopy. In order to investigate the Zn^{II} binding capability of the aminoacetate arms, the Eu^{III} analogue of **Gd-daa3** was synthesized with ^{13}C isotopic labeling of the aminoacetate groups. In the absence of Zn^{II}, no carbon shifts are visible because of the line-broadening effects of the paramagnetic Eu^{III} metal center when the aminoacetate arms are bound to Eu^{III} (Figure 3A). Upon the addition of Zn^{II} to the same sample, two peaks are seen in the ^{13}C NMR spectrum corresponding to the two carbon atoms on the aminocetates with shifts at 178 ppm for the carbonyl and 62 ppm for the methylene (Figure 3B). When bound to Zn^{II} and not bound directly to the Eu^{III} metal, the line broadening due to the paramagnetism is reduced, resulting in two carbon shifts from the ^{13}C-labeled aminoacetates that were not previously seen. These results provide

(23) Kropp, J. L.; Windsor, M. W. *J. Chem. Phys.* **1965**, *42*, 1599–1608.
(24) Horrocks, W. D.; Sudnick, D. R. *Acc. Chem. Res.* **1981**, *14*, 384–392.
(25) Quici, S.; Cavazzini, M.; Marzanni, G.; Accorsi, G.; Armaroli, N.; Ventura, B.; Barigelletti, F. *Inorg. Chem.* **2005**, *44*, 529–537.

Figure 3. (A) ^{13}C NMR in the absence of Zn^{II} of **Eu-daa3** and (B) ^{13}C NMR in the presence of 1 equiv of Zn^{II} with **Eu-daa3** providing evidence of the interaction of the aminoacetate groups with Zn^{II} and Eu^{III}.

direct evidence of the interaction of the aminoacetates with the Zn^{II} and Eu^{III} metal centers.

Discussion

The four complexes investigated in this study provide evidence of the mechanism of activation for Zn^{II}-activated contrast agents. The first of this series of Zn^{II}-activated contrast agents, **Gd-daa3**, has two aminoacetate arms that are proposed to vary metal-binding coordination upon the addition of Zn^{II}.[20] Three new complexes were synthesized in which the Zn^{II} binding groups are modified with one or two pyridyl groups (**Gd-apa3** and **Gd-dpa3**, respectively) or with the complete removal of one of the coordinating aminoacetate arms (**Gd-aa3**). Investigation of the relaxivities and q values determined that two structural requirements were necessary for the preparation of Zn^{II}-activated MRI agents. The first requirement is the presence of at least one aminoacetate to create a coordinatively saturated complex before binding of Zn^{II}. The second requirement is the need for at least two Zn^{II} coordination groups to effectively bind Zn^{II} and create a high-relaxivity state when Zn^{II} is present.

Evidence of the efficient reduction of water access with only one aminoacetate coordinating arm present is demonstrated by the low-relaxivity values of complexes **1−3** in the absence of Zn^{II}. The hydration numbers of **Tb-daa3** and

Tb-apa3 before the addition of Zn^{II} indicate a coordinatively saturated $q = 0$ complex. However, the high-relaxivity value of **Gd-dpa3** in the absence of Zn^{II} and the hydration number of **Tb-dpa3** are indicative of a coordinatively unsaturated structure in which water can access the Gd^{III} metal center, providing further evidence of the need for one aminoacetate to create a low-relaxivity complex. The slight decrease of relaxivity observed for **Gd-dpa3** in the presence of Zn^{II} may be due to a more rigid conformation that reduces the access of water to Gd^{III}. While the hydration numbers remain statistically unchanged for **Gd-dpa3** in the presence and absence of Zn^{II}, the observed decrease in relaxivity could be interpreted as a change in the second-shell solvation environment.

The second criterion is that Zn^{II} binding can only occur if there are at least two Zn^{II}-coordinating arms present. The addition of Zn^{II} increases the relaxivity by more than 100% for **Gd-daa3** and **Gd-apa3**. In the case of **Gd-aa3**, only one coordinating arm is available for Zn^{II} binding and can therefore not coordinate Zn^{II} to create a change in relaxivity in the presence of Zn^{II}. NMR spectroscopy of ^{13}C-labeled aminoacetates of **Eu-daa3** provides evidence of the Zn^{II} coordination to the aminoacetates to support the mechanism of activation presented in Figure 1, where a change in the coordination number from nine to eight is observed upon Zn^{II} binding.

A thorough understanding of the mechanism of Zn^{II} activation of the MRI contrast agent **Gd-daa3** described in this work is important for the development of new agents with a range of binding constants for Zn^{II}. We have determined that one of the aminoacetate arms can be modified with a variety of functional groups while still maintaining the ability to modulate q, which is necessary for activation of the contrast agent.